DEVELOPING WEARABLE BLOOD GLUCOSE METER USING RAMAN SPECTROSCOPY TECHNIQUE

by

Akraradet Sinsamersuk

A Dissertation Submitted in Partial Fulfillment of the Requirements for the Degree of Doctor of Engineering in Data Science and Artificial Intelligence

Examination Committee:	Dr. Chaklam Silpasuwanchai (Chairperson)
	Dr. Chutiporn Anutariya
	Dr. Attaphongse Taparugssanagorn
	Dr. Raffaele Ricco
Nationality:	Thai
Previous Degree:	Master of Engineering in Computer Science
	Asian Institute of Technology
	Pathum Thani, Thailand
Scholarship Donor:	Royal Thai Government

Asian Institute of Technology
School of Engineering and Technology
Thailand
August 2022

ABSTRACT

Continuous glucose monitoring (CGM) systems have been identified as a crucial component of successful glycemic management in diabetic patients (Lee, Probst, Klonoff, & Sode, 2021). Currently, the commercial CGM approach involves implanting a sensor (Keenan, Mastrototaro, Voskanyan, & Steil, 2009). Its minimally-invasive nature prevents the pervasiveness of monitoring glucose. The non-invasive approach such as Raman spectroscopy has been studied as a means to measure glycemic in vivo. Thus, wearable (continuous, non-invasive, pervasive) self-monitoring blood glucose (SMBG) is possible. However, wearable has its limitation and previous works do not study the aspect of this usage. Thus, a comprehensive comparison between measuring sites, measuring schemes, preprocessing techniques, and models is studied here. Furthermore, a prototype of wearable SMBG is developed and evaluated. We found that the wrist is the best site to measure glycemic. When use normalized 1125 cm^{-1}, it achieved $R^2 = 0.9$ with blood glucose. Our prototype measurement achieves correlation with blood glucose over $R^2 = 0.8$ comparable to reputable wearable SpO2 sensors in the market. Our results contribute to (1) the best site to measure glycemic in the human and measuring scheme, (2) effective preprocessing technique and model for predicting the glycemic, (3) prototyping the wearable SMBG using Raman spectroscopy.

CONTENTS

	Page
ABSTRACT	**ii**
LIST OF TABLES	**v**
LIST OF FIGURES	**vi**
CHAPTER 1 INTRODUCTION	**1**
1.1 Background of the Study	1
1.2 Statement of the Problem	2
1.3 Objectives	3
1.3.1 Study 1: Confirming the parameters	3
1.3.2 Study 2: Raman scattering of blood glucose study	4
1.3.3 Study 3: Designing and developing wearable blood glucose device	4
1.3.4 Study 4: Device Evaluation	4
1.4 Organization of the Study	4
CHAPTER 2 LITERATURE REVIEW	**5**
2.1 Glucose fingerprint	5
2.2 Measuring Sites	5
2.3 Preprocessing techniques and Data modeling	8
CHAPTER 3 METHODOLOGY	**9**
3.1 Study 1: Confirming the parameters	9
3.1.1 Equipment	9
3.1.2 Studying Measuring schemes	9
3.1.3 Data collection	9
3.1.4 Metric	10
3.2 Study 2: Raman scattering of blood glucose study	10
3.3 Data Collection	11
3.4 Preprocessing and Data Modeling	11
3.5 Metric	11
3.6 Study 3: Designing and developing wearable blood glucose device	11
3.7 Study 4: Device Evaluation	12

REFERENCES **13**

LIST OF TABLES

Tables **Page**

Table 2.1 Assignments of Raman peaks that are identified in the spectra of the microvessels and blood (Chaiken et al., 2001; Enejder et al., 2005; Lemler, Premasiri, DelMonaco, & Ziegler, 2014; Magnussen et al., 2017) 6

LIST OF FIGURES

Figures **Page**

Figure 2.1 Raman spectra of glucose solution at different concentration (Shao et al., 2012). 5

Figure 2.2 A trace of glucose fingerprint in Raman scattering of in vivo blood (Shao et al., 2012). 7

Figure 2.3 (**A**) Raman spectra of blood glucose obtained by subtracting two Raman signals (Kang et al., 2020). 7

Figure 2.4 (**A**) Blood glucose value with 1125 cm^{-1} relative intensity. (**B**) Concentration-dependent Raman relative intensities of glucose (1125 cm^{-1}) (Shao et al., 2012) 8

Figure 2.5 (**B**) Showing the linear relationship between normalized 1125 cm^{-1} with blood glucose ($R^2 = 0.94$) (Kang et al., 2020) 8

Figure 3.1 An example of wearable (*Measure blood oxygen levels on Apple Watch*, 2022). 11

CHAPTER 1
INTRODUCTION

1.1 Background of the Study

Continuous glucose monitoring (CGM) systems have been recognized as a key factor for effective glycemic control of diabetic patients (Lee et al., 2021). CGM refers to automatic, continuous (real-time or periodic) monitoring of users' glucose through invasive, minimally invasive (e.g., small incisions), and non-invasive means. To date, the acceptable and commercialized CGM approach is through sensor implantation, but it requires lengthy calibrations, sometimes unreliable and minimally-invasive (Keenan et al., 2009).

Non-invasive techniques through analyte (e.g., glucose solution, interstitial fluid (ISF)) analysis have attracted much interest. Optical-based methods were proven to yield superior results, achieving strong selectivity of glucose fingerprints on complex analytes such as blood (Alsunaidi, Althobaiti, Tamal, Albaker, & Al-Naib, 2021). Among the optical-based methods (e.g., far infrared to fluorescence spectroscopy), Raman spectroscopy appears promising due to its insensitivity to water (e.g., as compared to near-infrared) and its ability to accurately measure glucose quantitatively and transcutaneously (Kang et al., 2020). Anyhow, Raman spectroscopy comes with challenge, as is often confounded with fluorescence artifacts, but of which is commonly countered by adjusting the laser intensity or measuring schemes. The rise of Raman spectroscopy is also timely due to its recent advancement of laser technology (*Discover 50 years of Raman innovation by HORIBA*, 2018).

The use of Raman spectroscopy for measuring blood glucose can be dated back as far as 2005. Enejder et al. (2005) found a strong association ($R^2 = 0.83$) on Raman spectra between crystallized glucose and ISF measured at human forearm. Shao et al. (2012) confirmed a strong association ($R^2 = 0.91$) on Raman spectra between concentration on glucose solution and ISF measured at mouse ear. Kang et al. (2020) demonstrated a new approach to extract glucose scattering by subtracting two Raman signals from two different time points as a direct measurement of glucose in blood. In addition, they validated that to reliably measure the glucose concentration in blood, the glucose peak (1125cm^{-1}) should be normalized with protein and lipid peak (1450cm^{-1}). They

achieved an $R^2 = 0.91$ between actual glycemic and predicted glycemic using Raman spectra measured from a pig's ear. The measuring site is another important variable. Forearm (Enejder et al., 2005; Scholtes-Timmerman, Bijlsma, Fokkert, Slingerland, & Veen, 2014), thenar (Lundsgaard-Nielsen et al., 2018), and nail fold (Li et al., 2019) have been chosen as promising measurement sites. While González Viveros et al. (2022) indicates that the forearm is the most effective site when compared to the wrist and index finger, it remains unclear which site is the best due to varying equipment, parameters, and methodology (e.g., how to preprocess) across the papers. Due to the portability of wearables, there has also been some very recent attempt to deploy Raman spectroscopy on wearable (e.g., smartwatch) commercially *Quantum Operation Inc.* (2022) but the research is still in its infancy.

This research aims to build on previous work by (1) confirming the use of Raman scatterings for measuring blood glucose, (2) comparing models, and (3) developing the first wearable (continuous, non-invasive, pervasive) Raman-based self-monitoring blood glucose (SMBG) system, primarily for daily users for widespread use. The accuracy of the glycemic measurement should be comparable to that of the well-respected SpO2 wearable sensor (Apple Watch 6) of ($R^2 = 0.81$, $p < 0.001$) (Pipek, Nascimento, Acencio, & Teixeira, 2021). This justification was made because Raman spectroscopy was demonstrated to have at most 90% association with blood glucose. In addition, body movements may potentially confound the measurements, so it is advisable to set the objective for daily users rather than for clinical use.

1.2 Statement of the Problem

The difficulty of this work is brought on by the wearable's general limitations, limited power and battery. Therefore, the measuring site, scheme, and model have to be chosen carefully. In addition, comparing previous results is difficult since they all used different equipment, parameters, and methodology.

The measuring site (forearm, wrist, nail fold, and fingertip) may yield different Raman scattering signals. In terms of design, the wrist is the ideal site since it can be employed in the wearable such as smartwatches which are already widely daily driven and adopted. If other sites are chosen then another form of wearable has to be considered which will raise the usability question. Although the forearm is a superior option when compared to the wrist and fingertip in the indirect measurement (González Viveros et

al., 2022), proof of direct glucose measurement is absent. Furthermore, each site has a different skin structure, thus the appropriate measuring scheme should also be different. As a result, it is necessary to research the measuring sites and their optimal scheme in order to assess the direct glucose measurement and evaluate the sites based to their correlation with glycemic, Signal-to-noise ratio (SNR), and total measuring duration. The measuring scheme will be benchmarked with Apple Watch SpO2 sensor which uses a total measuring time of 15 seconds (*Measure blood oxygen levels on Apple Watch*, 2022).

The choice of model should be based on both resource consumption (model complexity) and accuracy (predictability). Earlier studies demonstrated that the normalized 1125 cm^{-1} has a linear relationship with in vivo blood glucose concentration ($R^2 = 0.95$) (Shao et al., 2012). However, the normalization-based works did not measure Raman from human subjects (Kang et al., 2020; Shao et al., 2012). Other works that involve human subjects use various preprocessing methods, such as principal component analysis (PCA) (Li et al., 2019) and self-organizing maps (SOM) (González Viveros et al., 2022). The aforementioned factors make it impossible to compare models. In addition, resource consumption should be assessed as its impacts the wearable battery life. Therefore, a thorough comparison of preprocessing and model selection is required.

1.3 Objectives

Our objective is to develop a wearable SMBG. To achieve this, we separate the project into four studies.

1.3.1 Study 1: Confirming the parameters

Objective: To study the measuring site and schemes.

Independent Variables:

1. Measuring Scheme
2. Measuring Site
    (a) Wrist
    (b) Forearm
    (c) Index fingertip
    (d) Index nail fold

Dependent Variables: Spectra peaks around 1125 cm^{-1} with the lowest total measuring time.

Outcome: Confirm the suited measuring site and scheme.

1.3.2 Study 2: Raman scattering of blood glucose study

Objective: Study Raman scattering of blood glucose and build a model to predict the glycemic for a wearable device.

Independent Variables: Raman scattering of blood

Dependent Variables: Glycemic

Outcome: The model that results in glycemic prediction correlation $R^2 > 0.8$ with actual glycemic, and resource usage.

1.3.3 Study 3: Designing and developing wearable blood glucose device

Objective: Design and develop a prototype of a wearable SMBG.

Outcome: A prototype.

1.3.4 Study 4: Device Evaluation

Objective: To evaluate the prototype, we redo Section 1.3.2 experiment with our prototype.

Independent Variables: Raman scattering of blood

Dependent Variables: Glycemic

Outcome: Prototype achieves glycemic prediction correlation $R^2 > 0.8$ with actual glycemic.

1.4 Organization of the Study

The document is organized as following. Chapter 2 as Literature Review and Chapter 3 as Methodology.

CHAPTER 2
LITERATURE REVIEW

We review the result of Raman spectra of amorphous glucose (glucose fingerprint) when combined with water (glucose solution) and blood (blood glucose). Then, we go into measuring sites and preprocessing techniques, and data modeling.

2.1 Glucose fingerprint

The "glucose fingerprint" is a characteristic Raman scattering spectrum that appears when glucose is present in the analyte. The Raman scattering in glucose solution (glucose and water) exhibits peaks at 796, 1060, 1125, and 1366 cm^{-1} (Figure 2.1). These peaks increase as a function of glucose concentration showing the quantitative property of Raman spectroscopy (Shao et al., 2012). The glucose fingerprint also exhibits in a more complex analyte as blood when measuring Raman scattering of ISF (Enejder et al., 2005; González Viveros et al., 2022; Kang et al., 2020; Scholtes-Timmerman et al., 2014) as show in Figure 2.4.

Kang et al. (2020) extracts the glucose fingerprint which has a peak at 1125 cm^{-1} from two noisy Raman signals. As a result, Raman spectroscopy can measure blood glucose.

2.2 Measuring Sites

Because the thickness of the human skin varies from place to place, Raman scattering measurements taken at several sites might provide varied results (González Viveros et al., 2022; Li et al., 2019). The glucose fingerprint signal will be stronger if the laser

Figure 2.1

Raman spectra of glucose solution at different concentration (Shao et al., 2012).

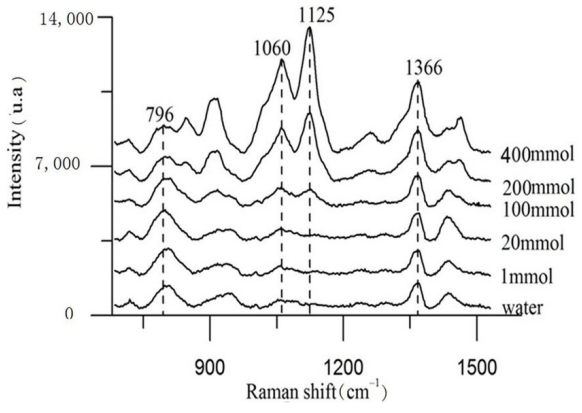

Table 2.1

Assignments of Raman peaks that are identified in the spectra of the microvessels and blood (Chaiken et al., 2001; Enejder et al., 2005; Lemler et al., 2014; Magnussen et al., 2017)

Peak Position (cm^{-1})		Assignments	Components
Microvessels	Blood		
650	643	P:C-S str	Ascorbic acid
758	752	ν_{15}	Trp
837	827	$\gamma 10$	Fructose
858	855	$\nu(C-C)$	Tyr, lac
885	-	-	-
902	898	p:C-C skeletal	Tyr
945	940	$\nu(C-C)$	Crtic acid
978	971	p: Skeletal vibr	Fibrin
1004	1004	ν-ring	Phe
1027	1026	$\delta(=C_bH_2)$asym	Lac
1130	1129	ν_5,	Lac
1163	1157	ν_{44}	Heme
1217	1212	$\nu_5+\nu_{18}$	Heme
1320	1321	p: CH2 twist	Try
1332	1341	ν_{41}	Trp
1424	1423	ν_{28}	Acetates
1448	1450	$\delta(=CH_2/CH_3)$	Trp
1551	1546	ν_{11}	Heme
1608	1603	$\nu(C=C)_{\text{venyl}}$	Heme
1660	1653	Amide I	Heme

Figure 2.2

A trace of glucose fingerprint in Raman scattering of in vivo blood (Shao et al., 2012).

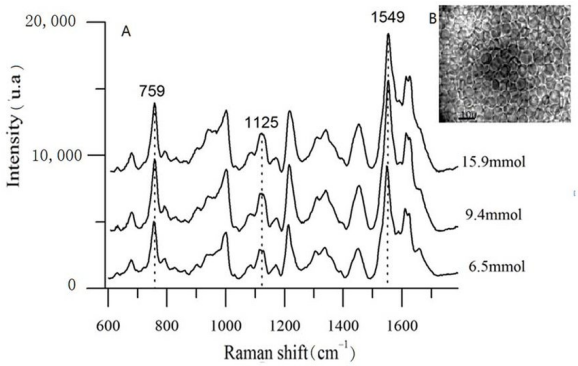

Figure 2.3

*(**A**) Raman spectra of blood glucose obtained by subtracting two Raman signals (Kang et al., 2020).*

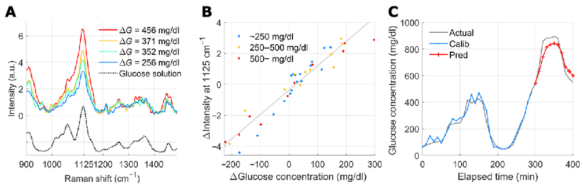

focuses on the blood vessels (Shao et al., 2012). Human skin consists of multiple layers called the stratum corneum (SC), epidermis, and dermis (Li et al., 2019). In most sites (e.g., wrist, forearm, fingertip), the assessed Raman signal is from ISF of SC and epidermis layer (Li et al., 2019). The following problems may arise when measuring glucose in ISF rather than blood, (1) ISF glucose is lag when compared to blood glucose (Cengiz & Tamborlane, 2009; Steil et al., 2005), (2) concentration of glucose in ISF is significantly lower than blood (O'Kane, 2012). As a result, the signal of glucose Raman scattering is weak (Li et al., 2019). A better strategy is to measure the Raman signal in areas where the laser can reach the dermis better. Because the dermis contains microvessels (Cutolo, Grassi, & Matucci Cerinic, 2003; Ingegnoli, Smith, Sulli, & Cutolo, 2018), if the site (nailfold) is picked carefully, we can obtain the glucose signal directly from the blood.

Li et al. (2019) reports the greater $R^2 = 0.98$ prediction correlation when use nailfold as a measuring site. The result is better than the forearm ($R^2 = 0.83$) (Enejder et al., 2005; Scholtes-Timmerman et al., 2014) and fingertip ($R^2 = 0.91$) (Oh et al., 2011). Recently, González Viveros et al. (2022) measures Raman glucose at forearm, wrist, and index fingertip and achieves the root-mean-square error (RMSE) of 56.31 ± 4.28,

Figure 2.4

*(**A**) Blood glucose value with 1125 cm^{-1} relative intensity. (**B**) Concentration-dependent Raman relative intensities of glucose (1125 cm^{-1}) (Shao et al., 2012)*

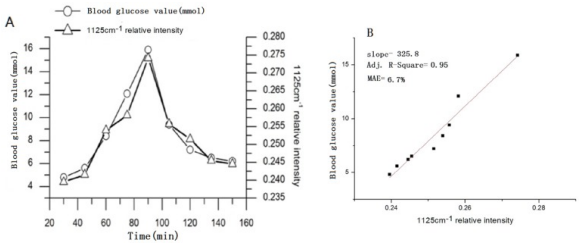

Figure 2.5

*(**B**) Showing the linear relationship between normalized 1125 cm^{-1} with blood glucose ($R^2 = 0.94$) (Kang et al., 2020)*

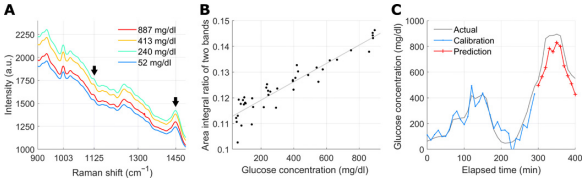

58.22 ± 1.03, and 56.65 ± 8.99 ml/dL respectively.

2.3 Preprocessing techniques and Data modeling

There are primarily two preprocessing options. Either extracting the features or utilize the complete Raman spectrum as an input. The full spectrum analysis pair with partial least squares (PLS) is widely used (Enejder et al., 2005; González Viveros et al., 2022; Kang et al., 2020; Scholtes-Timmerman et al., 2014). The results vary from $R^2 = 0.62$ (Kang et al., 2020), $R^2 = 0.83$ (Enejder et al., 2005; Scholtes-Timmerman et al., 2014), and RMSE of around 65 $\pm$ 0.4 ml/dL in González Viveros et al. (2022). The preprocessing can be done by hand-pick (Kang et al., 2020; Shao et al., 2012) or automatically (González Viveros et al., 2022; Li et al., 2019) pick the features. Hand-pick features were performed by normalizing the spectra with either protein and lipid peaks (1450 cm^{-1}) (Kang et al., 2020) or hemoglobin peaks (1549 cm^{-1}) (Shao et al., 2012). It is demonstrated that the normalized 1125 cm^{-1} has a linear correlation with in vivo blood glucose at $R^2 = 0.95$ (Shao et al., 2012). In Kang et al. (2020), normalized 911, 1060, 1125 cm^{-1} with 1450 cm^{-1} were utilized as inputs of the more complex multiple linear regression (MLR) which achieved $R^2 = 0.91$. The automatic feature extraction was demonstrated with PCA (Li et al., 2019) and SOM (González Viveros et al., 2022).

CHAPTER 3
METHODOLOGY

3.1 Study 1: Confirming the parameters

The purpose of this study is to clarify how measurement sites and schemes affect Raman spectra. The outcome of this study will be used to design the experiment in Section 3.2.

3.1.1 Equipment

The Raman instrument equipped with a 785 nm laser and 10x objective lens will be used to assess the Raman spectra. The Accu-Chek® Guide Meter is representing a standard blood glucose meter for SMBG (*Accu-Chek Guide meter | Accu-Chek*, 2022) and will be used for assessing glycemic.

3.1.2 Studying Measuring schemes

We will evaluate the Raman spectroscopy at four measurement sites: the wrist, forearm, index fingertip, and index nail fold. The measuring schemes will be put to the test to see which one produces the strongest scattering signal without introducing a fluorescence interference. The optimal measuring schemes will be used for the rest of the Raman scattering assessment.

3.1.3 Data collection

The Oral Glucose tolerance Test (OGTT) will be used to manipulate glycemic of the three healthy participants. The participants have to conduct fasting at least eight hours before the test. Once the participants arrived at the experiment area, they will be instructed to acclimate for 30 minutes. During the acclimation, instructor will repeat the experiment procedure. Both Raman Instrument and conventional SMBG equipment will be used to collect data at the interested measuring site. When the acclimation is completed, the first sample will be drawn. The participants begin the OGTT by consume a 250 ml of water containing 75 g of glucose in five minutes. Then, for the next two hours; (1) collecting Raman spectra at the interested measuring site every five minutes; (2) collecting blood sample at the interested measuring site every 20 minutes. In total, there will be 25 Raman samples and eight blood samples.

Each participant has to repeat the experiment until all four measuring sites are measured. The experiment has to be done on another day.

3.1.4 Metric

The subtraction of two Raman signals will be used to extract the glucose fingerprint. The remaining signal is the change of glucose concentration as showed in the following derivation.

The Raman spectra (RS) contains glucose fingerprint (G) and tissue spectra (T).

$$\mathrm{RS} = \mathrm{G} + \mathrm{T} \tag{3.1}$$

Then, the subtraction of two Raman signal can be represented as follows;

$$\Delta\mathrm{RS} = \mathrm{RS}_1 - \mathrm{RS}_2 \tag{3.2}$$

where RS_i is the Raman spectra measured at time i. Then, substituting Equation 3.2 with Equation 3.1 will derive the follows

$$\Delta\mathrm{RS} = \Delta\mathrm{G} + \Delta\mathrm{T} \tag{3.3}$$

Given the measuring site is the same, the tissue spectra will also be the same. Thus, ΔT is 0. Then, it is obvious that

$$\Delta\mathrm{RS} = \Delta\mathrm{G} \tag{3.4}$$

Therefore, the best measuring site is the one that produces the greatest correlation between ΔG and the actual changes in blood glucose.

3.2 Study 2: Raman scattering of blood glucose study

The purpose of this study is to model the relationship between Raman spectra and blood glucose. The same equipment from Section 3.1 will be used. The measuring site and scheme are chosen based on the result of Section 3.1.

Figure 3.1

*An example of wearable (*Measure blood oxygen levels on Apple Watch*, 2022).*

3.3 Data Collection

The same data collection and experiment procedure from Section 3.1 will also be used. In this study, we increase the number of participants to 15 participants. The participants shall be from three different age groups (5 each from 20 to 35 years, 36 to 50 years, and 51 to 65 years).

A total of $15 \times 25 = 375$ Raman samples and $15 \times 8 = 120$ blood samples are collected.

3.4 Preprocessing and Data Modeling

The acquired Raman spectra will be normalized by their intensity of 1450 or 1549 cm^{-1}. Thus, there are three preprocessing options: (1) without normalization, (2) normalize with 1450 cm^{-1}, and (3) normalized with 1549 cm^{-1}. The Linear Regression (LR) model will be used to assess the linearity of 1125 cm^{-1} with glucose concentration. The MLR model with 911, 1060, 1125 cm^{-1} as inputs we will use for multivariate analysis. As a baseline model, full spectrum with PLS will also be employed.

In total, there will be $3 \times 3 = 9$ combinations to compare.

3.5 Metric

The model performance will be assessed using the Pearson correlation. Additionally, resource usage during prediction will be tracked.

3.6 Study 3: Designing and developing wearable blood glucose device

Objective: Design and develop a prototype of a wearable SMBG.

Outcome: A prototype.

3.7 Study 4: Device Evaluation

Objective: To evaluate the prototype, we redo Section 3.2 experiment with our prototype.

Independent Variables: Raman scattering of blood

Dependent Variables: Glycemic

Outcome: Prototype achieves glycemic prediction correlation $R^2 > 0.8$ with actual glycemic.

REFERENCES

Accu-chek guide meter | accu-chek. (2022). https://www.accu-chek.com/meters/guide-meter/specs. ([Online; accessed 2022-11-09])

Alsunaidi, B., Althobaiti, M., Tamal, M., Albaker, W., & Al-Naib, I. (2021). A review of non-invasive optical systems for continuous blood glucose monitoring. *Sensors*, *21*(20), 6820.

Cengiz, E., & Tamborlane, W. V. (2009). A tale of two compartments: interstitial versus blood glucose monitoring. *Diabetes technology & therapeutics*, *11*(S1), S–11.

Chaiken, J., Finney, W. F., Knudson, P. E., Peterson, K. P., Peterson, C. M., Yang, X., & Weinstock, R. S. (2001). Noninvasive blood analysis by tissue-modulated nir raman spectroscopy. In *Visualization of temporal and spatial data for civilian and defense applications* (Vol. 4368, pp. 134–145).

Cutolo, M., Grassi, W., & Matucci Cerinic, M. (2003). Raynaud's phenomenon and the role of capillaroscopy. *Arthritis & rheumatism*, *48*(11), 3023–3030.

Discover 50 years of raman innovation by horiba. (2018). https://www.horiba.com/int/scientific/technologies/raman-imaging-and-spectroscopy/history-of-raman-spectroscopy/. ([Online; accessed 2022-11-13])

Enejder, A. M., Scecina, T. G., Oh, J., Hunter, M., Shih, W., Sasic, S., ... Feld, M. S. (2005). Raman spectroscopy for noninvasive glucose measurements. *Journal of biomedical optics*, *10*(3), 031114.

González Viveros, N., Castro-Ramos, J., Gomez-Gil, P., Cerecedo-Núñez, H., Gutierrez-Delgado, F., Torres Rasgado, E., ... Flores-Guerrero, J. (2022, 09). Quantification of glycated hemoglobin and glucose in vivo using raman spectroscopy and artificial neural networks. *Lasers in Medical Science*, 1-13. doi: 10.1007/s10103-022-03633-w

Ingegnoli, F., Smith, V., Sulli, A., & Cutolo, M. (2018). Capillaroscopy in routine diagnostics: potentials and limitations. *Current Rheumatology Reviews*, *14*(1), 5–11.

Kang, J. W., Park, Y. S., Chang, H., Lee, W., Singh, S. P., Choi, W., ... others (2020). Direct observation of glucose fingerprint using in vivo raman spectroscopy. *Science Advances*, *6*(4), eaay5206.

Keenan, D. B., Mastrototaro, J. J., Voskanyan, G., & Steil, G. M. (2009). Delays in minimally invasive continuous glucose monitoring devices: A review of current tech-

nology. *Journal of Diabetes Science and Technology*, *3*(5), 1207-1214. Retrieved from https://doi.org/10.1177/193229680900300528 (PMID: 20144438) doi: 10.1177/193229680900300528

Lee, I., Probst, D., Klonoff, D., & Sode, K. (2021). Continuous glucose monitoring systems - current status and future perspectives of the flagship technologies in biosensor research -. *Biosensors and Bioelectronics*, *181*, 113054. Retrieved from https://www.sciencedirect.com/science/article/pii/S0956566321000919 doi: https://doi.org/10.1016/j.bios.2021.113054

Lemler, P., Premasiri, W., DelMonaco, A., & Ziegler, L. (2014). Nir raman spectra of whole human blood: effects of laser-induced and in vitro hemoglobin denaturation. *Analytical and bioanalytical chemistry*, *406*(1), 193–200.

Li, N., Zang, H., Sun, H., Jiao, X., Wang, K., Liu, T., & Meng, Y. (2019, 04). A noninvasive accurate measurement of blood glucose levels with raman spectroscopy of blood in microvessels. *Molecules*, *24*, 1500. doi: 10.3390/molecules24081500

Lundsgaard-Nielsen, S., Pors, A., Banke, S., Henriksen, J., Hepp, D., & Weber, A. (2018, 05). Critical-depth raman spectroscopy enables home-use non-invasive glucose monitoring. *PLOS ONE*, *13*, e0197134. doi: 10.1371/journal.pone.0197134

Magnussen, L., Hvid, L., Hermann, A., Hougaard, D., Gram, B., Caserotti, P., & Andersen, M. (2017). Testosterone therapy preserves muscle strength and power in aging men with type 2 diabetes—a randomized controlled trial. *Andrology*, *5*(5), 946–953.

Measure blood oxygen levels on Apple Watch. (2022). https://support.apple.com/guide/watch/blood-oxygen-apdaf17aa5ef/watchos. ([Online; accessed 2022-11-09])

Oh, J., Cho, S., Oh, H., Ku, Y., Shim, B., Kim, M., ... Miller, D. R. (2011). The high-quality spectral fingerprint of glucose captured by raman spectroscopy in non-invasive glucose measurement. In *Optical diagnostics and sensing xi: Toward point-of-care diagnostics; and design and performance validation of phantoms used in conjunction with optical measurement of tissue iii* (Vol. 7906, pp. 67–74).

O'Kane, M. J. (2012). *The accuracy of point-of-care glucose measurement* (Vol. 49) (No. 2). SAGE Publications Sage UK: London, England.

Pipek, L. Z., Nascimento, R. F. V., Acencio, M. M. P., & Teixeira, L. R. (2021). Comparison of spo2 and heart rate values on apple watch and conventional commercial oximeters devices in patients with lung disease. *Scientific Reports*, *11*(1), 1–7.

Quantum operation inc. (2022). https://quantum-op.co.jp/en. (Online; accessed 2022-11-09)

Scholtes-Timmerman, M., Bijlsma, S., Fokkert, M., Slingerland, R., & Veen, S. (2014, 07). Raman spectroscopy as a promising tool for noninvasive point-of-care glucose monitoring. *Journal of diabetes science and technology*, *8*. doi: 10.1177/1932296814543104

Shao, J., Lin, M., Li, Y., Li, X., Liu, J., Liang, J., & Yao, H. (2012). In vivo blood glucose quantification using raman spectroscopy. *PloS one*, *7*(10), e48127.

Steil, G., Rebrin, K., Hariri, F., Jinagonda, S., Tadros, S., Darwin, C., & Saad, M. (2005). Interstitial fluid glucose dynamics during insulin-induced hypoglycaemia. *Diabetologia*, *48*(9), 1833–1840.